

CLASSIFIER FOR REMOTELY SENSED IMAGERY USING KOHONEN'S SELF-ORGANIZING FEATURE MAP WITH REGION GROWING

Mitsuyoshi TOMIYA

Seikei University, Department of Applied physics
Musashino-shi, Kichijyoji-Kitamachi 3-3-1, Tokyo 180-8633, Japan
tomiya@apm.seikei.ac.jp

KEY WORDS: Remotely Sensed Imagery, Self-Organizing Feature Map, Region Growing, Polar coordinate System

ABSTRACT

Applying the region growing to the Kohonen's self-organizing feature map, a non-supervised classifier for remotely sensed imagery data is proposed. If the self-organizing feature map is made large enough, i.e., the size is 50×50 sites, it can be considered as a kind of image itself. Then the region growing method is effective to separate the feature map into several segments, which represent the categories in the remotely sensed data. Introducing the polar coordinate system in the feature space, this method is more effective than on the Cartesian coordinate system.

1 THE KOHONEN'S SELF-ORGANIZING FEATURE MAP

The Kohonen's self-organizing feature map is a kind of neural networks, which is aimed at competitive learning (Kohonen (1982, 1997)). The competitive learning is one of the typical non-supervised learning procedures for computers. The neural network consists of two layers; the first one is the input layer and the second is the competition layer (Figure 1). It can treat n -dimensional ($n > 1$) input data and the input layer has n units. The competition layer is usually a two-dimensional grid which has $m \times m$ sites. Their coordinates are represented as (x, y) ($x, y = 0, 1, \dots, m - 1$). On each site there is a unit of the competition layer. If input is given, units in the first layer get values that correspond to the input data. Then units in the second layer compete to be the only winner unit. Actually the learning is done by the weights on the bonds between the units on the first and the second layer. The initial values of them can be chosen to be just random.

The first step of the learning is to calculate the difference value $|E - U_i| = \sqrt{\sum_j (e_j - u_{ij})^2}$, where

we define an input data as $E = [e_1, e_2, \dots, e_n]$ and the weights on the bonds from the input layer to a unit in the second layer as $U_i = [u_{i1}, u_{i2}, \dots, u_{in}]$ ($i = m^2$). The unit whose difference value is the minimum is the winner unit u_c . The second step is to update the weights. We upgrade not only the weights connected to the winner unit but also the weights to units in the neighborhood of the winner unit. If u_c is located at (x_c, y_c) , its neighborhood is defined as

$$x_c - d < x < x_c + d, \quad y_c - d < y < y_c + d, \quad (1)$$

where the size of the neighborhood is controlled by the parameter

$$d = d_0 \left(1 - \left(\frac{t}{T} \right)^f \right) + 1, \quad (2)$$

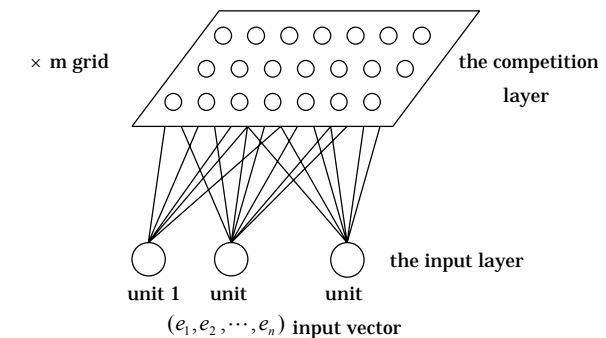


Figure 1. Basic Structure of Kohonen's Self-Organizing Feature Map

and T is the maximum time for the learning and $t(=0,1,2,\dots,T)$ is a discrete time. The neighborhood is determined as almost the whole size of second layer at first and then gradually shrink to one unit. The weights are upgraded as

$$u_{ij}^{new} = u_{ij}^{old} + \Delta u_{ij}, \text{ where } \Delta u_{ij} = \begin{cases} \alpha(e_j - u_{ij}^{old}) & : i \text{ is inside the neighborhood} \\ 0 & : \text{otherwise} \end{cases} \quad (3)$$

Here α is the learning coefficient and also decreasing

$$\alpha = \alpha_0 \left(1 - \left(\frac{t}{T} \right)^f \right) \quad (4)$$

We choose $d_0 = m/3$, $\alpha_0 = 1/2$ and $T = 15$. We also choose the competition layer as square shape, then also the neighborhood square. We check several values of exponent f in Equation 2 and Equation 4 for the neighborhood and the learning coefficient such as 1/2 and 1/4 etc., though, the final result is essentially the same at least for our purpose.

Thus above linearly decreasing function is considered to be enough. At each time t every n -dimensional pixel value of the image is inputted to the network one by one. After the learning process, the set of the weights called the self-organizing feature map.

We choose the pseudo color image (R=TM3, G=TM4, B=TM1) of Hachirogata at Akita prefecture, Japan, which was scanned by the Thematic Mapper of Landsat 5 at 21 August 1989 as the remotely sensed data (Figure 2). Therefore the input layer has only three units ($n=3$). Hachirogata has distinct and characteristic land cover and it is suitable for a test area. It was once a lagoon and was reclaimed over 30 years ago. Then we get the result of the learning, i.e., the self-organizing feature map as Figure 3 from an initial random map. Each cell on Figure 3 represents the weights on the bonds from the input layer to each unit on the competition layer as a RGB value. As a result the regions which may correspond to the typical categories in the remotely sensed image data are located near the corners and



Figure 2. Pseudo color image of Hachirogata , Japan

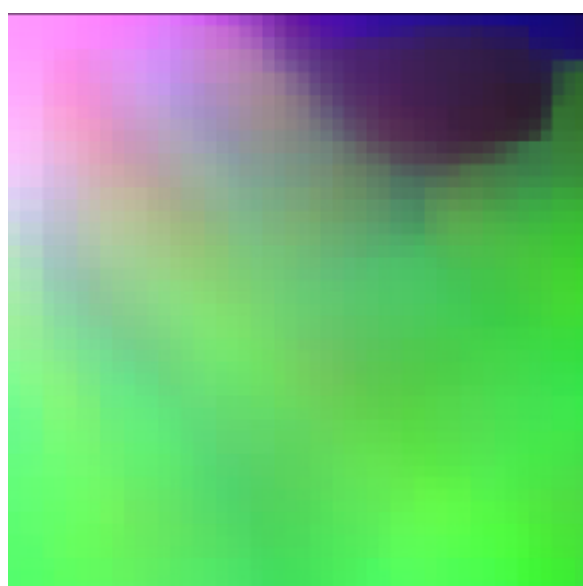


Figure 3. The feature map of Hachirogata after the learning

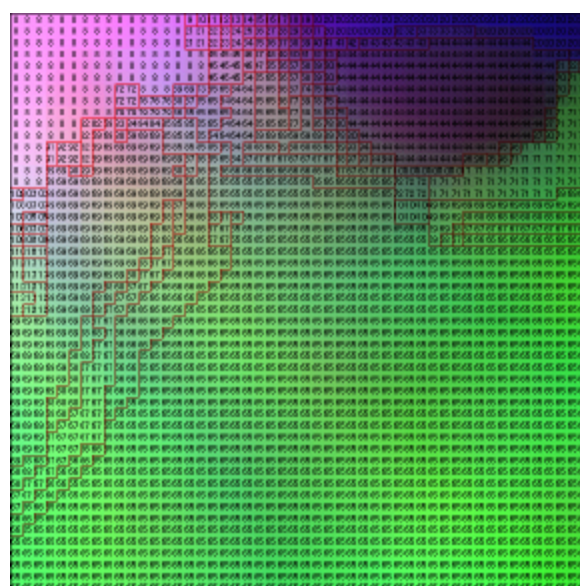


Figure 4. The feature map of Hachirogata after the region growing

fringes of the feature map. There is the gradation of their mixture around the center of the map. As mentioned above its result is found to be robust in changing learning parameters T , d_0 , α_0 and f , as far as it converges.

2 THE REGION GROWING

The region growing method is originally developed to extract uniform regions in the imagery by computer automatically. Here it is adopted to abstract the category information from the feature map. This time every unit in the feature map must be classified to some category. After the learning the feature map has the clusters, which show representative contents of land cover. To do this the feature map must have enough size to make this method work well. In other words, the map must be large enough to be treated as an image for the region growing method. We choose $m=50$ to satisfy this condition.

In this method whether adjoining units belong to the same region or not is dependent on the threshold value of the difference between them. Several variations of the region growing we are trying to get better results in this paper, however, they are all based on the simple and naive growing method. If the difference between weights of a unit in the fringe of the region and weights of unit next to the fringe unit in the feature space is smaller than some threshold value, then the next unit belongs to the region. This procedure continues until every unit in the feature map belongs to some region. Type-A is the simple region growing method. In type-B the definition of the distance in the feature space is redefined on the polar coordinate system. This is based on the idea that the physical information of the data is much easier to grasp on the polar coordinate system: (r, ϑ, φ) than the Cartesian coordinate system: (x, y, z)

$$x = r \cos \theta \sin \varphi, \quad y = r \sin \theta \sin \varphi, \quad z = r \cos \varphi,$$

as we will mention in section 3. Here we define the difference as $\ell = \sqrt{(r-r')^2 + (\theta-\theta')^2 + (\varphi-\varphi')^2}$. Type-C does the region growing in two steps. At first we see the difference of the fringe unit and the next unit in the radial direction. If the radial difference is under the threshold value for the radial direction, then we observe the angular difference measured from the origin of the feature space. If the angular difference is also under the threshold for the angular direction, we add the unit to the region. Roughly speaking, it may be a kind of the mixture of the region growing and the multi-level slice classifier. The last methods sound a little conventional rather than rigorous, however, the results are fairly good. They may have different result if initial point for the region growing is different. Therefore we have to check the robustness of the result, by changing the order of selecting the initial unit to grow the regions. In Figure 4 we show the result of the region growing of type-A. Actually after the region growing, there are 65 to 304 regions in the feature map. If we adjust the threshold value decrease the number of regions, then the feature map becomes inadequate. For example even two water bodies: Japan sea and the reservoir around the reclaimed land are melted into one region. Most of small regions surround the larger typical categories' regions. Therefore we add smaller regions to adjoining larger region, until they become seven fundamental regions: 1.Sea, 2.Lagoon, 3.Vegetation, 4.Forest, 5.Farm, 6.Soil and 7.Built-up land.

3 THE POLAR COORDINATE SYSTEM TO THE FEATURE SPACE

We use the distance in the feature space as the difference between the weights of the units in the feature map. Introducing the polar coordinate system to the feature space, the distance of the remotely sensed data can be defined more properly (Tomiya et. al. (1995,1996)). It means that the position of the data should be considered in the aspect of the distance from the origin of feature space and angular positions in the space. Roughly speaking the remotely sensed data consist of three kinds of information. One is the irradiance which includes the sun altitude, sun distance, atmospheric

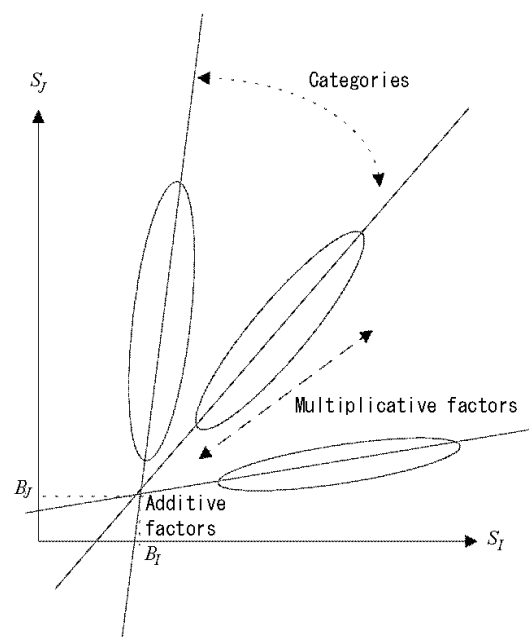


Figure 5. Schematic distribution of remotely sensed data in the feature space.

absorption etc.. Another one is the information of physical characteristics of land cover, i.e. categories. The former becomes mainly the multiplicative factor of the remotely sensed data and the later is what we wish to investigate. Additive factor is the other contents of the data, e.g., path radiance etc..

Due to slope etc., if solar irradiance is varied, the same objects seem to have different spectral characteristics. But reflectances of surface objects must not be varied, then these data forms linear distribution from the origin, because this multiplicative factor affects every band data almost equivalently. This is the reason that data distributed radially. They originate from the point near the origin not exactly from the origin. It means that they have offsets, which may involve mainly path radiance. It is also supported by the fact that offset is larger in the band of shorter wavelength.

More rigorous explanation of the nature of radial distribution will be following. Assume that there exist N -bands. The spectral signal of band I ($I=1,2,\dots,N$) would be presented with respect to the reflectance r_I^a of ground object of category a as

$$S_I^a = A_I r_I^a + B_I, \quad (5)$$

where A_I is a multiplicative factor by the sun radiance etc. and B_I is an additive factor by path radiance etc.. If the ground objects belong to the same category, ratios of the reflectances are determined the same. Therefore as for band I and band J

$$\frac{r_J^a}{r_I^a} = \frac{S_J - B_J}{S_I - B_I} \cdot \frac{A_I}{A_J} = d_{IJ}^a = \text{const} \quad (6)$$

The primary of the multiplicative factor would be the difference of sun radiance: sunshine-shade and slopes etc., because it works equally on each band, the ratio between A_I and A_J can be fixed. Other multiplicative factor such as the transmittance of the atmosphere is assumed to remain the same in the whole scene. Thus we put $c_{IJ}^a = d_{IJ}^a \cdot A_J / A_I$ (=const) and Equation 6 becomes

$$c_{IJ}^a (S_I - B_I) = S_J - B_J \quad (7)$$

If Equation 7 holds for all I, J ($I \neq J$), it forms a line (a one-dimensional object) in N -dimensional characteristic space. Moreover the major part of the additive factor is said to be path radiance, which is due to the dispersion by water vapor and aerosol in the air. Therefore it can be assumed that the offset is roughly common to all ground objects. Then all lines, which represent categories respectively, converge the point in the vicinity of the origin of the feature space. The point represents the offsets and will be called the new origin. The data distribute radially from the new origin. The line extends from the new origin shows the category and the distance from the new origin implies the multiplicative factor.(Figure 5)

Concerning remotely sensed multispectral data, if ratios of reflectances of a ground objects are identical, those reflectance themselves can also expect to be identical. The possibility that all ratios of those DN value accidentally coincide is relatively low.

4 RESULTS AND DISCUSSIONS

Type-C has the best result (Figure 9). It shows the potential to separate soil and built-up land and it can extract the road in the middle of rice field most properly. But it still has 304 regions just after the region growing. The ordinary region growing method with the Cartesian distance: Type-A is the second best (Figure 7). The threshold value of the region growing is 9.00 and it has 95 regions after the region growing. Unfortunately the classification by Type-B is worst (Figure 8). The threshold value is 4.0 and it has 65 regions. It cannot even separate the two typical water regions in the image: Japan sea and the reservoir around the reclaimed land, which is the remnant of the lagoon.

Type-B is the worst so far, however, it still has the potential to become much better. Because the result of Type-C has high quality and it handles the radial distance and the angle measured from the origin of the feature space between two units in the feature map. Even, only with radial distance, the result doesn't look very bad, though it cannot distinguish between soil and built-up land almost by the definition of the method (Figure 10). It doesn't use the angular information in the feature map. It implies that the distance defined by the polar coordinate system should work. We previously confirmed the effectiveness of the polar coordinate system in the maximum likelihood classifier, the minimum distance classifier, etc. (Tomiya et. al. (1996)). It means that we should include the concept of the variances of the each category's distribution that are fully utilized in the most of classifiers of multi-dimensional data. Even clustering methods such as ISODATA (Ball and Hall, (1965)) method use the variances of clusters. Toward this

purpose, we are studying the distance $\ell = \sqrt{C(r-r')^2 + (\theta - \theta')^2 + (\varphi - \varphi')^2}$, introducing the constant C to adjust the effect of the radial distance and the angular distance in the feature space. There is no reason to use different weights for two angular directions. We have checked that the learning result of the self-organizing feature map is stable with respect to the change of the learning parameters. Therefore, apparently, it is to be solved that many regions remain after the region growing. In this paper we use the naive region growing as the base of our growing method, however, these are more sophisticated region growing method whose results may be more precise (Muerle and Allen (1968), Brice and Fennema (1970), Tomita et. al. (1996),...). We should also try them to improve our classifier.

1 Sea	2 Lagoon	3 Vegetation	4 forest	5 Farms	6 soil	7 built-up land
-------	----------	--------------	----------	---------	--------	-----------------

Figure 6. Table of land cover

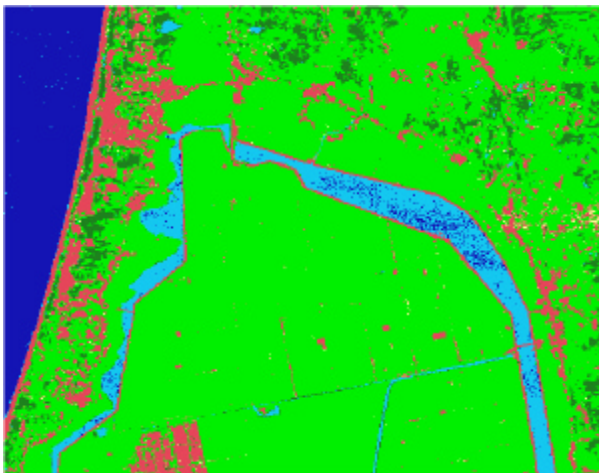


Figure 7. Result of classification :Type-A

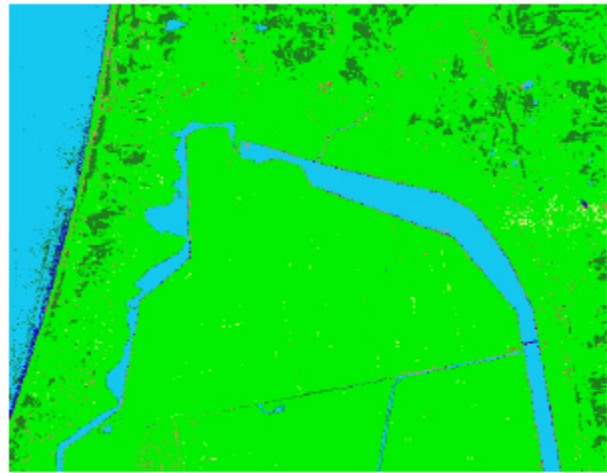


Figure 8. Result of classification: Type-B

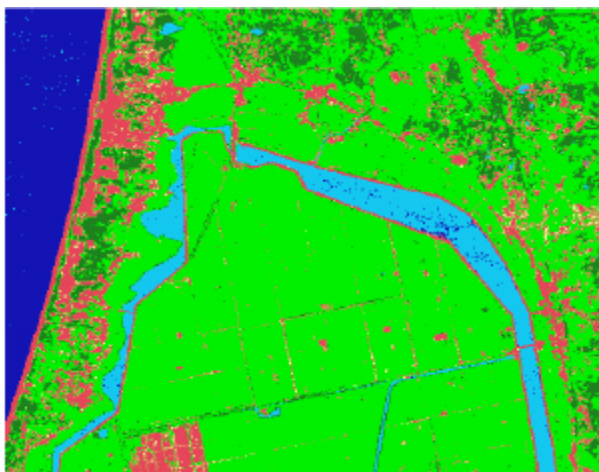


Figure 9. Result of classification: Type-C

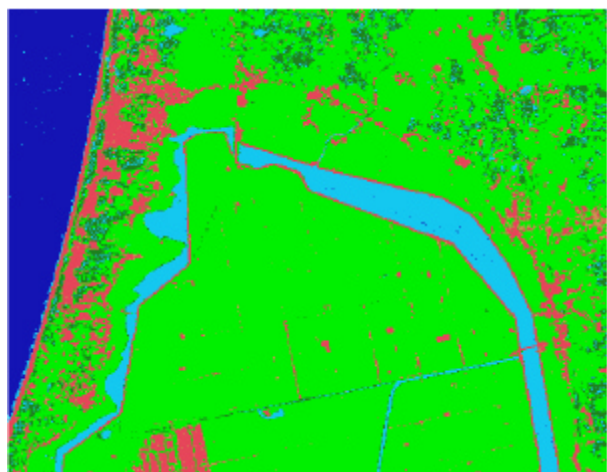


Figure 10. Using only radial distance in the feature space for the region growing, the result is better than Type-B.

ACKNOWLEDGEMENTS

I would like to thank my students and especially Mr. Masatoshi Sugiyama for his devoted and tireless support.

REFERENCES

- Kohonen T., 1982. Self-Organized Formation of Topologically Correct Feature Maps, *Biol. Cybern.*, 43, pp.59-69
- Kohonen T., 1997. *Self-Organizing Maps*, 2nd ed., Springer, New York
- Tomiya M., Ishiguro H., Nakajima Y., Yamaguchi M., Toyota H., 1995. On Category Classification of Remotely Sensed Multispectral Image by Linear Algebraic Method, *Journal of the Remote Sensing Society of Japan*, 15(4), pp.10-21, in Japanese
- Tomiya M., Ishiguro H., Nakajima Y., Toyota H., 1996. Classification of Categories on Remote Sensing Multispectral Image Data by the Angular Distribution in the Feature Space, *Journal of the Remote Sensing Society of Japan*, 16(1), pp.59-67, in Japanese
- Ball G. H., Hall D. J., 1965. *ISODATA-Novel Method of Data Analysis and Pattern classification*, Menlo Park, California, Stanford Research Institute
- Muerle J. L., Allen D. C., 1968. Experimental Evaluation of Techniques for Automatic Segmentation of Objects in A Complex Scene, in *Pictorial Pattern Recognition*, Thompson, Washinton, D. C., pp.3-13
- Brice C. R., Fennema C. L., 1970. Scene analysis using regions, *Artificial Intelligence*, 1(3), pp205-226
- Tomita F., Shirai Y., Tsuji S., 1979. Description of Textures by Structural Analysis, in *Proc. 6th IJCAI*, Tokyo, pp.884-889